Spin-dependent variable range hopping and magnetoresistance in $Ti_{1-x}Co_xO_2$ and $Zn_{1-x}Co_xO$ magnetic semiconductor films

2006 J. Phys.: Condens. Matter 18 10469

(http://iopscience.iop.org/0953-8984/18/46/014)

INSTITUTE OF PHYSICS PUBLISHING JOURNAL OF PHYSICS: CONDENSED MATTER

J. Phys.: Condens. Matter **18** (2006) 10469–10480 doi:10.1088/0953-8984/18/46/014

Spin-dependent variable range hopping and magnetoresistance in $Ti_{1-x}Co_xO_2$ and $Zn_{1-x}Co_xO$ magnetic semiconductor films

Shi-shen Yan[1,2,3], J P Liu[2], L M Mei[1], Y F Tian[1], H Q Song[1], Y X Chen[1] and G L Liu[1]

[1] School of Physics and Microelectronics, and National Key Laboratory of Crystal Materials, Shandong University, Jinan, Shandong 250100, People's Republic of China
[2] Department of Physics, The University of Texas at Arlington, Box 19059, Arlington, TX 76019, USA

E-mail: shishenyan@yahoo.com

Received 27 August 2006
Published 3 November 2006
Online at stacks.iop.org/JPhysCM/18/10469

Abstract

Magnetic transport properties in $Ti_{1-x}Co_xO_2$ and $Zn_{1-x}Co_xO$ magnetic semiconductors have been studied experimentally and theoretically. A linear relation of $\ln\rho$ versus $T^{-1/2}$ (ρ is sheet resistance and T is temperature), which shows different slopes and intersections at different magnetic fields, was observed experimentally in the low temperature range. The spin-dependent variable range hopping model has been proposed by taking into account the electron–electron Coulomb interaction and the spin–spin exchange interaction in the same frame, which can well describe the observed magnetic transport properties in $Ti_{1-x}Co_xO_2$ and $Zn_{1-x}Co_xO$ magnetic semiconductors.

1. Introduction

Electrical transport and magnetoresistance (MR) in many material systems have been extensively studied due to their significant importance not only in fundamental physics but also in technological applications. It is well known that the electrical transport of a doped nonferromagnetic semiconductor can be described by the Mott's variable range hopping (VRH) theory ($R \propto \exp\{(T_0/T)^{1/4}\}$) if there is no interaction between the carriers [1]. If there exists Coulomb interaction between the carriers, the electrical transport of the doped nonferromagnetic semiconductor obeys the Efros's VRH theory ($R \propto \exp\{(T_0/T)^{1/2}\}$) [2].

For most doped nonmagnetic semiconductor materials (a disordered system), the MR was usually found at low temperature, and several mechanisms of the MR were proposed [3–12]. Generally speaking, the electrical transport in the Anderson localization region is usually through the VRH mechanism, and the MR in doped semiconductors can originate from the

[3] Author to whom any correspondence should be addressed.

orbital effects [3] and spin effects [4–12]. The orbital effects on the MR are well known [3]. By contrast, the spin effects on the MR are very complicated. When intra-impurity interaction (double occupancy model) is taken into account, the polarization of the electron spins can block some of the hopping processes, leading to an exponentially increased resistance (positive MR) [4, 5]. As for the large negative spin-dependent MR observed at very low temperature in the Anderson localization regime, several scenarios have been suggested, such as localization length variation caused by the change of Fermi energy relative to the mobility edge due to the Zeeman splitting in magnetic field [7, 11, 12], destruction of the bound magnetic polarons by magnetic field [6], spin dependent VRH due to the spin–spin exchange interaction [8–10] and so on.

Recently, magnetic semiconductors have been extensively studied for their great importance in spintronics devices. For ferromagnetic semiconductors, the carriers are spin polarized, and thus not only the Coulomb interaction between the charges of the electrons but also the exchange interaction between the spins of the electrons may influence the electrical transport properties. It was reported that a large negative MR was observed in $Zn_{1-x}Co_xO$ [13] and $Ti_{1-x}Co_xO_2$ [14] inhomogeneous magnetic semiconductor films, which was attributed to spin-dependent VRH in the presence of Coulomb interaction and exchange interaction. The inhomogeneous $Ti_{1-x}Co_xO_2$ (or $Zn_{1-x}Co_xO$) magnetic semiconductor means that the distribution of Co atoms in the $Ti_{1-x}Co_xO_2$ compound (or $Zn_{1-x}Co_xO$) is inhomogeneous on the subnanometre scale, but no detectable pure Co metal clusters were found by transmission electron microscopy (TEM), x-ray diffraction (XRD), energy dispersive x-ray spectroscopy (EDS), or x-ray photoelectron spectroscopy (XPS) [14]. However, there is no quantitative theoretical electrical transport model which has taken into account the spin polarization and the exchange interaction in the ferromagnetic semiconductors. In this paper, the magnetic transport of the $Ti_{1-x}Co_xO_2$ and $Zn_{1-x}Co_xO$ magnetic semiconductors were experimentally studied, and a theoretical model of spin-dependent VRH in the presence of Coulomb interaction and exchange interaction was established to explain the observed magnetic transport phenomena.

2. Experimental results

The $Zn_{1-x}Co_xO$ magnetic semiconductor films were prepared on glass substrates by alternately sputtering very thin Co layers and ZnO layers for 60 periods (the nominal structure is [Co 0.6 nm/ZnO y nm]$_{60}$) in Ar and background O_2 gas at room temperature. Due to the atomic interdiffusion between the alternately deposited very thin Co and ZnO layers, the nominal [Co 0.6 nm/ZnO y nm]$_{60}$ structure formed the $Zn_{1-x}Co_xO$ magnetic semiconductor single-layer films with nanometre grains. The average grain size observed by TEM is about 4–6 nm [13]. The $Ti_{1-x}Co_xO_2$ magnetic semiconductor films were also prepared on glass substrates by a similar process, but they are in an amorphous state [14]. The detailed growth procedure, microstructures and magnetic properties of $Ti_{1-x}Co_xO_2$ and $Zn_{1-x}Co_xO$ magnetic semiconductor films have been reported previously [13, 14]. In order to make our electrical transport model easy to understand, we give a brief description of these experimental results of $Ti_{0.24}Co_{0.76}O_2$ (70 nm in thickness) and $Zn_{0.28}Co_{0.72}O$ (71 nm in thickness) magnetic semiconductor films in this part.

The magnetic properties were measured by superconducting quantum interference devices (SQUIDs) from 4.5 K to room temperature. The magnetic field is applied in the film plane. Figure 1(a) shows hysteresis loops of the $Ti_{0.24}Co_{0.76}O_2$ magnetic semiconductor measured at 5 and 290 K, respectively. The room temperature ferromagnetism is clearly shown by the coercivity, remanence, and low saturation field. Therefore, the Curie temperature is above room temperature. Since the film is in a metastable state, we did not measure the Curie temperature

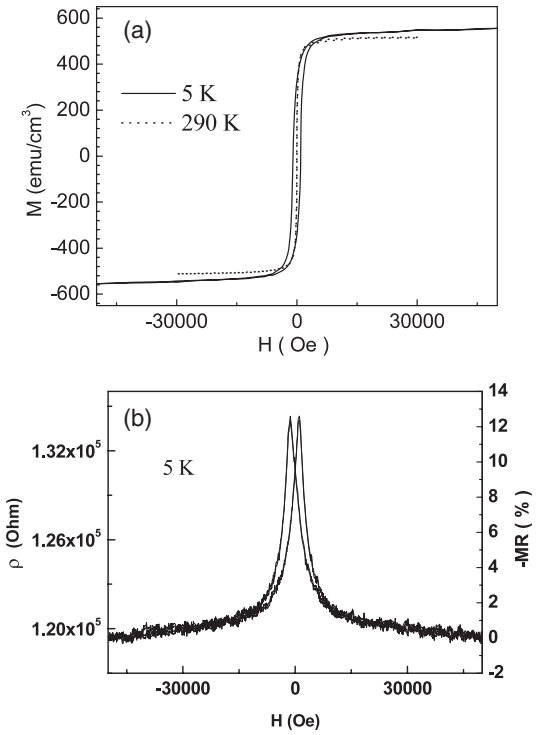

Figure 1. (a) Magnetization hysteresis loops of the as-deposited $Ti_{0.24}Co_{0.76}O_2$ film (70 nm in thickness) measured at 5 and 290 K, respectively. (b) Dependence of the sheet resistance ρ and the MR ratio on the magnetic field measured at 5 K. The applied magnetic field is in the film plane.

at high temperature. The magnetization is in the film plane and there is no magnetic anisotropy in the film plane. Similar ferromagnetic properties were also found in the $Zn_{1-x}Co_xO$ magnetic semiconductor [13].

The electrical transport properties were measured by Van der Pauw configuration from 4.5 K to room temperature. The applied field is in the film plane. Figure 1(b) shows the dependence of the sheet resistance ρ and the MR ratio on the magnetic field, measured at 5 K. The MR ratio is defined as $\mathrm{MR}(H, T) = \{R(H_S, T) - R(H, T)\}/R(H_S, T) \times 100\%$, where $R(H, T)$ is the resistance at the field H and the temperature T, and $R(H_S, T)$ is the resistance at the saturation field H_S (here it is replaced by the maximum applied field in the measurements). The $Ti_{0.24}Co_{0.76}O_2$ sample shows a large negative MR at a relatively small field, such as 12.5% at 5 K. The ρ–H curve in figure 1(b) shows an obvious magnetic hysteresis behaviour, which corresponds to the magnetic hysteresis of the M–H loop in figure 1(a) measured at 5 K. The peak resistance in figure 1(b) was observed around the magnetic field which corresponds to the coercivity in figure 1(a). When the magnetization gradually becomes saturated with increasing field, the resistance also shows a trend to saturation. This implies that the negative MR observed in figure 1(b) is related to spin-dependent electrical transport effects. Similar MR behaviour was also found in the $Zn_{1-x}Co_xO$ magnetic semiconductor [13]. However, the ρ–H curve in figure 1(b) is quite different from those observed in dilute ZnO-based [15, 16] and TiO_2-based [17–19] magnetic semiconductors, where the ρ–H curves usually show a positive MR or complicated behaviour without any magnetic hysteresis. Although the shape of the ρ–H curve in figure 1(b) is similar to that observed in conventional granular systems with giant

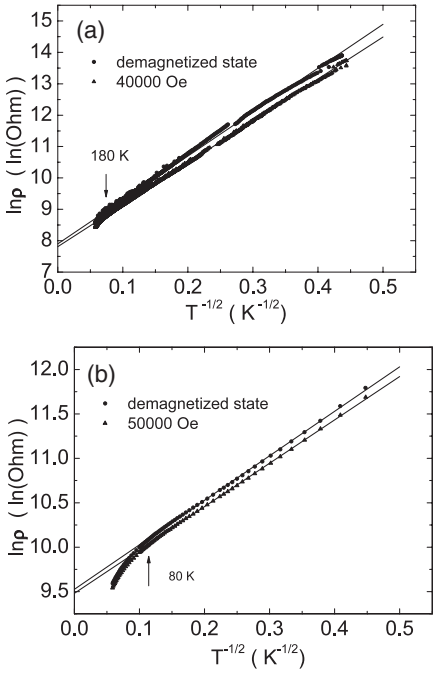

Figure 2. The dependence of ln ρ on $T^{-1/2}$ for (a) $Zn_{0.28}Co_{0.72}O$, and (b) $Ti_{0.24}Co_{0.76}O_2$ magnetic semiconductor films, where the intersection $\ln\{\rho_0/(1 + p^2\langle\cos\theta\rangle)\}$ and the slope $\langle T_0\rangle^{1/2}$ can be obtained from the extrapolated theoretical fitting lines. In (a), the intersection and the slope are respectively 7.898 ln(Ohm) and 13.87 $K^{1/2}$ without field, and they are 7.814 ln(Ohm) and 13.36 $K^{1/2}$ at $H = 40\,000$ Oe. In (b), they are 9.527 ln(Ohm) and 5.003 $K^{1/2}$ without field, and 9.480 ln(Ohm) and 4.880$K^{1/2}$ at $H = 50\,000$ Oe. The applied magnetic field is in the film plane.

magnetoresistance (GMR) or tunnelling magnetoresistance (TMR), a careful analysis in the following reveals that the MR in figure 1(b) cannot be attributed to the GMR or TMR effects of the granular systems.

Figures 2(a) and (b) show the temperature dependence of the sheet resistance of the $Zn_{0.28}Co_{0.72}O$ and $Ti_{0.24}Co_{0.76}O_2$ magnetic semiconductors on the ln ρ–$T^{-1/2}$ scale (sheet resistance ρ and temperature T), which were measured in different magnetic fields. In figure 2, the circles and triangles represent the experimental data, and the solid lines are theoretical fittings according to equation (10) (which will be described in detail in sections 3 and 4). The experimental results indicate that ln ρ versus $T^{-1/2}$ in the magnetic field and without field (the demagnetized state) is linear in the low temperature range (below 180 K in figure 2(a) and below 80 K in figure 2(b)).

The large negative MR which was found in the $Zn_{0.28}Co_{0.72}O$ and $Ti_{0.24}Co_{0.76}O_2$ magnetic semiconductors with high Co concentrations is different from the conventional GMR, TMR, CMR, AMR, and the positive MR in $Zn_{1-x}Co_xO$ and $Ti_{1-x}Co_xO_2$ with low Co concentrations. In the as-deposited films, we did not find the positive MR and AMR effects. It is well known that in the disordered semiconductor systems the $R \propto \exp\{(T_0/T)^{1/2}\}$ relation is called Efros's variable range hopping resistance [2]. However, the mechanism of the large negative MR of the ferromagnetic semiconductor in the variable range hoping region is still less known. We believe that it can be explained as the spin-dependent variable range hopping [8, 9]. In the ferromagnetic semiconductor system, there is strong spin–spin exchange interaction between

the carrier spins in addition to electron–electron Coulomb interaction between the carrier charges. In the magnetic field, the spins tend to align parallel, and the spin–spin exchange energy becomes small. As a result, the variable range hopping electrons have a lower resistance, showing spin-dependent variable range hopping and large negative magnetoresistance. In the following parts, a quantitative theoretical model which can well describe the observed experimental results is established.

3. Theoretical model and formula

Here we consider a system with compositional inhomogeneity on the subnanometre scale, such as $Zn_{1-x}Co_xO$ [13] and $Ti_{1-x}Co_xO_2$ [14] inhomogeneous magnetic semiconductors. As mentioned above, the inhomogeneous $Ti_{1-x}Co_xO_2$ (or $Zn_{1-x}Co_xO$) magnetic semiconductor means that the distribution of Co atoms in the $Ti_{1-x}Co_xO_2$ compound (or $Zn_{1-x}Co_xO$) is inhomogeneous on the subnanometre scale but no detectable pure Co metal clusters were found by TEM, XRD, EDS, and XPS. On the other hand, even if the films consist of tiny amorphous or nanocrystal Co metal grains (<20 Å in diameter) embedded in the oxide host (ZnO or TiO_2), the granularity effects on the electrical transport can be ignored [20, 21]. This can be understood from two aspects. First, according to Sheng *et al* [20], the charging electrostatic energy E_c of a tiny grain can be much larger than the thermal energy k_BT in the low temperature range, and this is not beneficial to the tunnelling between two grains if there exist other conducting paths, such as VRH. Second, according to Kim *et al* [21], the hopping length (of the order of 100 Å) of the VRH process in the low temperature range can be much larger than the tiny grain size, and hence the inhomogeneous composite system (with tiny grains) can be considered homogeneous for the VRH transport. In this sense, even if there are undetectable Co metal grains in magnetic semiconductor films, they do not influence the following analysis of the VRH transport.

It is well known that ZnO is a natural n-type semiconductor due to the existence of O vacancies and Zn interstitials. In the $Zn_{1-x}Co_xO$ magnetic semiconductor, there are many defects such as O vacancies, Zn interstitials, and doped Co atoms. The defect levels can supply weakly localized s, p carriers of the charges (n-type) near the Fermi level, which are responsible for the semiconducting transport. In this system, there exists a spin–spin exchange interaction between the s, p carriers and the strongly localized d electrons of Co. There also exists direct d–d exchange interaction between the neighbour Co atoms due to the high Co concentration. Therefore, local Co atoms may establish local ferromagnetic order and even long-ranged ferromagnetic structure through the RKKY (due to s, p–d exchange interaction) interaction and direct d–d exchange interaction between the neighbour Co atoms. In this case, the observed ferromagnetism in the $Zn_{1-x}Co_xO$ (and also in the $Ti_{1-x}Co_xO_2$) magnetic semiconductors is intrinsic ferromagnetism, rather than the ferromagnetism from metal Co clusters.

From the viewpoint of the electrical transport, the compositional inhomogeneity can produce strong local potential and lead to Anderson localization of the carriers near the Fermi level. For the magnetic Anderson localization system, the localized carriers should be spin polarized, and can 'feel' not only the local electrical potential fluctuation but also the local magnetic potential fluctuation. It has been shown that the electrical transport and magnetoresistance of the $Zn_{1-x}Co_xO$ and $Ti_{1-x}Co_xO_2$ magnetic semiconductors are related to the spin-dependent variable range hopping. The hopping carriers should be weakly localized s, p carriers near the Fermi level. The spin-dependent variable range hopping is mainly determined by the energy difference ΔE between the initial occupied i state and the final vacant j state of the hopping process, which is related to the effective interactions between two carriers in the magnetic semiconductor system.

In order to describe spin-dependent features of the variable range hopping, the spin–spin exchange interaction between the carrier spins and electron–electron Coulomb interaction between the carrier charges should be taken into account in the same frame. In this magnetic Anderson localization system, the Coulomb interaction $E_{co} = e^2/\varepsilon r$ between two localized carriers is significant, where $r = |\mathbf{r}_i - \mathbf{r}_j|$ is the distance between the two carriers in the states i and j, and ε is the dielectric constant.

Supposing the Hund's coupling is strong, the spin of a weakly localized s or p carrier is coupled to the spin of its nearest local Co atom. In this case, two carriers at a long distance can show an effective spin–spin exchange interaction through the surrounding Co atoms which have formed local ferromagnetic order. In the low temperature range, the carrier should hop a large distance to find a small energy difference ΔE between the initial occupied state and the final vacant state. Therefore, the effective spin–spin exchange interaction between two carriers which is related to the long distance hopping process at low temperature should be long ranged. If we assume that the long-ranged effective spin–spin exchange interaction between two carriers analogizes the RKKY interaction with its magnitude proportional to $1/r$ for a large distance in one dimension [22], it can take the form of $E_{ex} = -(J/r)\cos\theta$, where θ is the angle between the spin $\mathbf{S}_i$ in the i state and $\mathbf{S}_j$ in the j state at the distance r, and J/r is the effective coupling coefficient between the two carriers. For the hopping process of large distance r, exchange interaction may be mainly related to the spins in the hopping path if the relaxation is neglected. In this sense, the exchange interaction picture of one dimension is reasonable.

In this system, the total interaction E_{to} between the two carriers is the sum of the electron–electron Coulomb energy and spin–spin exchange energy, i.e.

$$E_{to} = E_{co} + E_{ex} = e^2/\varepsilon r - J\cos\theta/r. \tag{1a}$$

If we introduce the effective dielectric constant ε_{eff}, where $1/\varepsilon_{eff} = 1/\varepsilon - J\cos\theta/e^2$, we can rewrite equation (1*a*) as

$$E_{to} = E_{co} + E_{ex} = e^2/\varepsilon r - J\cos\theta/r = e^2/\varepsilon_{eff} r. \tag{1b}$$

In the Anderson localization system, the electrical transport is caused by carrier hopping from the initial localized occupied state to the end vacant state due to thermal activation. We consider two states i and j, which in the ground state are occupied and vacant respectively. In real space, the i state with one electron and its positive charge background shows charge neutrality, and the vacant j state also shows charge neutrality. Neglecting the relaxation of the system, the electron hopping from the i state to the j state will make the i state show one positive charge (hole) in real space due to the left positive charge background and make the j state show one electron. Thus an electron–hole pair is created in the hopping process. According to equation (1*a*) of the total interaction energy of two electrons E_{to}, it is easy to obtain that the total interaction energy of the electron–hole pair is $-E_{to}$. Following the work of Efros [2], if we introduce the energy of one-particle excitation E_i for the electron in state i, and E_j for the electron in state j, the energy increase of the system (defined as the excitation of an electron–hole pair) by the transfer of an electron from state i to state j should satisfy

$$\omega_{ij}(i \to j) = E_j - E_i - E_{to} \geqslant 0. \tag{2}$$

Since the excitation energy of this electron–hole pair is related to the spin–spin exchange interaction, we may call it a spin electron–hole pair. Equation (2) means that the single electron will overcome the energy $\Delta E = E_j - E_i$ to hop, i.e.

$$\Delta E = E_j - E_i \geqslant E_{to} = e^2/\varepsilon_{eff} r. \tag{3}$$

In the spirit of the original work by Mott [1], Efros [2] and Hamilton [23], and taking into account the influence of the relative direction of the spins on the tunnelling probability [24], the

electron tunnelling resistance between two localized states whose wavefunctions fall off with distance as $\exp(-2\alpha r)$ is dominated by the following equations:

$$\rho_{ij} = \{\rho_0/(1 + p^2 \cos\theta)\} \exp(2\alpha r) \exp(\Delta E/k_B T) \tag{4a}$$

where

$$p = (D_\uparrow - D_\downarrow)/(D_\uparrow + D_\downarrow) \tag{4b}$$

$$\alpha = \{2m^*(V - E_F)/\hbar^2\}^{1/2}. \tag{4c}$$

In equations (4*a*)–(4*c*), ρ_0 is a prefactor of the resistance which is mainly related to the material, p is the polarization ratio of the localized electron near the Fermi energy E_F, $1/\alpha$ is the localization length of the electron near the Fermi level, k_B is the Boltzmann constant, D_σ ($\sigma = \uparrow, \downarrow$) is the density of states near the Fermi energy E_F for electrons with spin σ, m^* is the effective electron mass, $V - E_F$ is the tunnelling potential (V) barrier height relative to the Fermi level E_F, and $\hbar$ is the Planck constant.

Putting expression (3) into equation (4*a*), and minimizing ρ_{ij} for the optimum hopping distance r at the given temperature T, we obtain

$$r = (e^2/2\alpha\varepsilon_{eff}k_B T)^{1/2} \tag{5}$$

which gives

$$\rho_{ij} = \{\rho_0/(1 + p^2 \cos\theta)\} \exp(T_0/T)^{1/2} \tag{6}$$

and

$$T_0 = 8e^2\alpha/\varepsilon_{eff}k_B = 8e^2\alpha/\varepsilon k_B - 8\alpha J \cos\theta/k_B. \tag{7}$$

For the whole system, the spins of the localized states may have their own local magnetization easy axes, so the angle θ may have a distribution and varies with the applied magnetic field. As an approximation, the hopping resistance of the whole system ρ can be expressed as follows:

$$\rho = \{\rho_0/(1 + p^2\langle\cos\theta\rangle)\} \exp(\langle T_0\rangle/T)^{1/2} \tag{8}$$

and

$$\langle T_0\rangle = (8e^2\alpha/k_B)\{1/\varepsilon - (J/e^2)\langle\cos\theta\rangle\} \tag{9}$$

where $\langle\cos\theta\rangle$ means the average value of $\cos\theta$.

Equation (8) can be rewritten as follows:

$$\ln\rho = \ln\{\rho_0/(1 + p^2\langle\cos\theta\rangle)\} + \langle T_0\rangle^{1/2} T^{-1/2} \tag{10}$$

which means that $\ln\rho$ versus $T^{-1/2}$ is a straight line with the intersection $\ln\{\rho_0/(1+p^2\langle\cos\theta\rangle)\}$ and the slope $\langle T_0\rangle^{1/2}$.

If we further suppose the easy axes of the localized ferromagnetic states are random in the film, we can obtain $\langle\cos\theta\rangle = m^2$, where m is the reduced magnetization of the whole system. In particular, although there is local spontaneous magnetization, the net magnetization of the whole system is zero in the demagnetized state (the as-deposited film without applying any magnetic field), i.e. $\langle\cos\theta\rangle = m^2 = 0$. In the magnetic saturation state, all the local magnetization is along the direction of the applied field, i.e. $\langle\cos\theta\rangle = m^2 = 1$. According to the definition of the MR ratio and equations (8) and (9), we can obtain the following expression of MR ratio from the demagnetization state to the magnetic saturation state:

$$\mathrm{MR} = 1 - (1 + p^2) \exp\{[(8e^2\alpha/\varepsilon k_B)^{1/2} - (8e^2\alpha/\varepsilon k_B - 8\alpha J/k_B)^{1/2}]/T^{1/2}\}. \tag{11}$$

4. Theoretical fitting to experimental results

Figures 2(a) and (b) also show the theoretical fitting to the experimental results. The experimental results indicate that $\ln\rho$ versus $T^{-1/2}$ is linear in the low temperature range (below 180 K in figure 2(a) and below 80 K in figure 2(b)), which can be well fitted by equation (10). Assuming $\langle\cos\theta\rangle = 0$ for the demagnetized state of $Zn_{0.28}Co_{0.72}O$, from the intersection and the slope of the extrapolated theoretical fitting line without field in figure 2(a), we can obtain $\rho_0 = \exp(7.898) = 2692\ \Omega$, and $8e^2\alpha/\varepsilon k_B = 192.38$ K. On the other hand, assuming $\langle\cos\theta\rangle = 1$ for the high magnetic field of 40 000 Oe, we can further obtain $P = 29.6\%$ and $8\alpha J/k_B = 13.78$ K. From these data, it is easy to get $E_{ex}/E_{co} = (-J\cos\theta/r)/(e^2/\varepsilon r) = (-13.78/192.38)\cos\theta \leqslant 7.2\%$.

For the same reason, the following parameters can be deduced from the fittings in figure 2(b) for the $Ti_{0.24}Co_{0.76}O_2$ magnetic semiconductor: $\rho_0 = \exp(9.527) = 13\,726\ \Omega$, $8e^2\alpha/\varepsilon k_B = 25.030$ K, $P = 21.9\%$, $8\alpha J/k_B = 1.216$ K, and $E_{ex}/E_{co} \leqslant 4.86\%$. It is reasonable that the effective exchange energy E_{ex} is less than a few per cent of the Coulomb energy E_{co} for both $Zn_{0.28}Co_{0.72}O$ and $Ti_{0.24}Co_{0.76}O$ magnetic semiconductors. However, we could not obtain the values of the Coulomb energy E_{co} and the effective exchange energy E_{ex} since the dielectric constant ε and the localization length $1/\alpha$ of the electrons near the Fermi level are not known yet. Figures 2(a) and (b) also indicate that in the high temperature range the experimental data deviate from the straight lines, i.e. the variable range hopping described by equation (10). The deviation from the variable range hopping is caused by the nearest-neighbour hopping or activation to a mobility edge in the high temperature range.

In order to further check the theoretical electrical transport model described by equation (10), Figures 3(a)–(c) show the experimental m–H curve, the theoretical ρ–H curve calculated by equation (10), and the experimental ρ–H curve together as a comparison. The theoretical ρ–H curve in figure 3(b) was directly calculated by equation (10), using the fitting parameters obtained in figure 2(b), i.e. $\rho_0 = \exp(9.527) = 13\,726\ \Omega$, $8e^2\alpha/\varepsilon k_B = 25.030$ K, $P = 21.9\%$, and $8\alpha J/k_B = 1.216$ K. $\langle\cos\theta\rangle = m^2$ was also used, where m is the experimental value shown in figure 3(a). In figure 3(a), the reduced magnetization m varies quickly in the low field range ($H < 10\,000$ Oe) as the field increases, and then m gradually approaches saturation in the high field range. Correspondingly, in figures 3(b) and (c) the sheet resistance ρ–H curves show a stiff decrease in the low field range, and a very slow decrease in the high field range. Moreover, the resistance peak positions of the ρ–H curve in figure 3(b) correspond to the coercivity positions in figure 3(a). It is clear that the theoretical ρ–H curve in figure 3(b) is in good agreement with the experimental results in figures 3(a) and (c).

5. Discussion and conclusions

The main assumption in our theoretical transport model is the function form of the effective spin–spin exchange interaction $E_{ex} = -(J/r)\cos\theta$, which analogizes the RKKY interaction with its magnitude proportional to $1/r$ for a large distance in one dimension [22]. It is well known that the exchange interactions in magnetic systems can show various function forms, depending on the origins of the exchange interactions. But it is worthy of mention that the $1/r$ dependence of the function in equation (1*a*) is a proper function form to deduce the linear dependence of $\ln\rho$ on $T^{-1/2}$ in equations (8)–(10). Good agreement between the experimental results and theoretical fittings (see figures 2 and 3) by equations (8)–(11) supports our assumption that the effective exchange energy can take the form of $E_{ex} = -(J/r)\cos\theta$ at least as a good approximation. In contrast, other function forms of the exchange interaction cannot deduce the $T^{-1/2}$ dependence of the resistance, so they are contradictory with the observed experimental results.

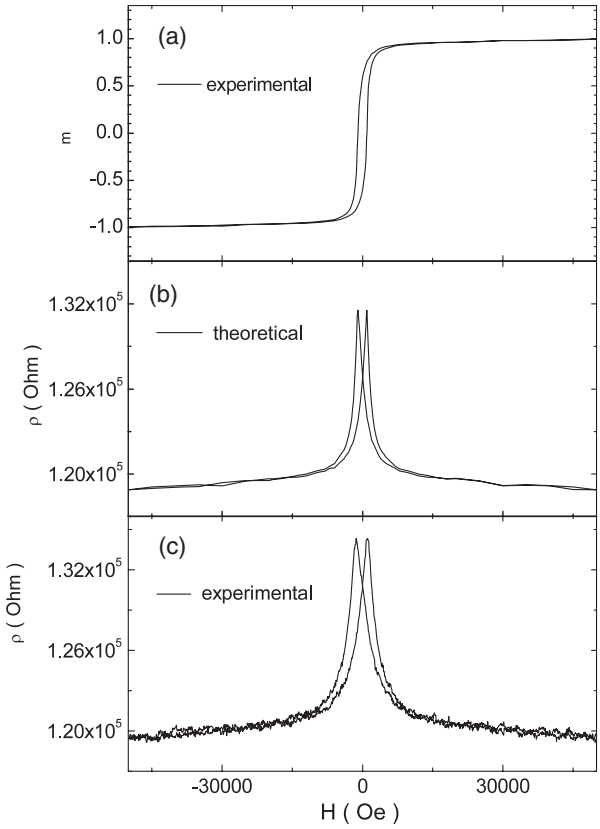

Figure 3. Direct comparison among the experimental m–H curve, the theoretical ρ–H curve, and the experimental ρ–H curve measured at 5 K for the $Ti_{0.24}Co_{0.76}O_2$ magnetic semiconductor film. (a) The experimental m–H curve redrawn from the M–H curve in 1(a), (b) the theoretical ρ–H curve calculated by equation (10), and (c) the experimental ρ–H curve redrawn from 1(b).

Equation (8) as the hopping resistance of the whole system is an approximation, which is not strict in mathematics. A conventional way to obtain the hopping resistance of the whole system is the percolation theory, which takes into account all the conducting paths with different distances r and angles θ. However, equation (8) is accurate enough to describe the experimental results. Therefore, we have not given a more detailed description by percolation theory.

The linear relation of $\ln\rho$ versus $T^{-1/2}$ was also found in a wide temperature range for the metal–insulator granular system with a wide distribution of grain sizes [20, 24–28]. According to the work of reference [20],

$$\ln\rho = \ln\rho_{0g} + T_{0g}^{1/2}T^{-1/2} \tag{12}$$

$$T_{0g} = 8sE_c\alpha/k_B \tag{13}$$

$$E_c = (e^2/\varepsilon d)\{(2s/d)/(1/2 + s/d)\} \tag{14}$$

$$\alpha = \{2m^*(V - E_F)/\hbar^2\}^{1/2}. \tag{15}$$

Here ρ_{0g} is a prefactor of the resistance of the granular system, s is the insulating spacing distance between the metal grains (tunnelling distance), d is the diameter of the metal grains ($s + d$ is equal to the distance between the centres of the two grains), and E_c is the charging energy. By the way, equations (15) and (4c) are the same in the two different cases.

It is worthy of note that several features of the electrical transport are obviously different between the present magnetic semiconductor and metal–insulator system. First, in the hopping transport theories for the metal–insulator system (equations (12)–(15)), the term $T_{0g} = 8sE_c\alpha/k_B$ does not vary with the applied field, but the experimentally observed values in figure 2 indeed depend on the applied magnetic field. Second, for the metal–insulator granular system, the linear relation of $\ln\rho$ versus $T^{-1/2}$ was usually found in a wide temperature range, such as 40–300 K in Co–TiO_2 [27] and 20–400 K in Ni–SiO_2 [20] granular films. The deviation from the $T^{-1/2}$ relation in the high temperature range observed in figures 2(a) and (b) cannot be explained by the electrical transport in the metal–insulator granular system, but it can be explained by the deviation from the variable range hopping which is caused by the nearest-neighbour hopping or activation to a mobility edge in the high temperature range. Third, the temperature dependence of the MR ratio described by equation (11) was also not experimentally found or predicted in the metal–insulator granular system [24–26], but it is in good agreement with the MR of the $Ti_{0.24}Co_{0.76}O_2$ magnetic semiconductor film in the low temperature range, as shown in figure 4(c) of [14]. In all, the spin-dependent variable range hopping observed in figure 2 is not related to the metal–insulator granular system.

Fitting the temperature dependence of the resistance in the demagnetized state of $Zn_{0.28}Co_{0.72}O$ by equation (12), we get $T_{0g} = 8sE_c\alpha/k_B = 192.38$ K. Assuming that the system is a Co–ZnO metal–insulator granular system with Co spherical metal grains embedded in insulator ZnO, just like the case of the Ni–SiO_2 granular film [28], it is physically reasonable for $\varepsilon = 10\varepsilon_0$ (ε_0 is the vacuum dielectric constant), $\alpha = \{2m^*(V - E_F)/\hbar^2\}^{1/2} = 10^8$ cm^{-1}. Combining equations (12)–(15), it is deduced that $s/d = 0.02$. Furthermore, supposing that a reasonable value of the insulating spacing (s) should be at least 4–6 Å, the diameter (d) of the metal grains should be at least 200–300 Å. However, such large Co metal clusters were not found at all [13]. Therefore, it is hard to explain the electrical transport properties observed in figure 2 by characteristics of a metal–insulator granular system.

It is worth comparing the MR behaviour between the Co–ZnO metal/semiconductor granular films and the $Zn_{1-x}Co_xO$ magnetic semiconductor films when they have the same atomic ratio of Co atoms to Zn atoms. Due to the thermal nonequilibrium growth process, the as-deposited magnetic semiconductor films are in the metastable state. Since the solubility of the Co element in ZnO oxide is very low under thermal equilibrium conditions, the Co element can be gradually separated from the as-deposited metastable $Zn_{1-x}Co_xO$ matrix to form granular composite film (such as Co–ZnO granular film) by proper annealing. Figure 4(a) is the TEM image of the annealed $Zn_{0.28}Co_{0.72}O$ film. The annealed film is composed of two kinds of grain of 10–30 nm in size. The composition of the grains can be detected by EDX. The black ones are Co grains and the grey ones are remanent $Zn_{1-x}Co_xO$ matrix. It is noticed that after some pure Co grains have precipitated the remanent matrix is $Zn_{1-x}Co_xO$ grains.

Figure 4(b) shows the ρ–H curve (or MR) of the annealed $Zn_{0.28}Co_{0.72}O$ film measured at 4.5, 20, and 50 K, respectively. The MR of the annealed samples is very complicated. When the temperature is above 50 K, all the MR effects are negligibly small (not shown in figure 4). As the temperature is below 50 K, there is a small negative magnetoresistance in the low magnetic field (<3000 Oe). In the high field range (>3000 Oe), the behaviour of the MR of the annealed sample is quite different from that of the as-deposited sample. At low temperature, such as 4.5 K, the resistance increases with the magnetic field (positive MR) in a high field (3000–23 000 Oe), and then decreases in higher field (>23 000 Oe). The MR does not show any sign of saturation even at 60 000 Oe field. At 20 K, the resistance only shows a small increase with increasing field from 3000 to 60 000 Oe. At 50 K, the positive MR disappears and only a very small negative MR (−0.84%) in the low field range remains. Similar phenomena were found in ZnO-based [15, 16], TiO_2-based [17–19], and SnO_2-based [29] magnetic semiconductors of

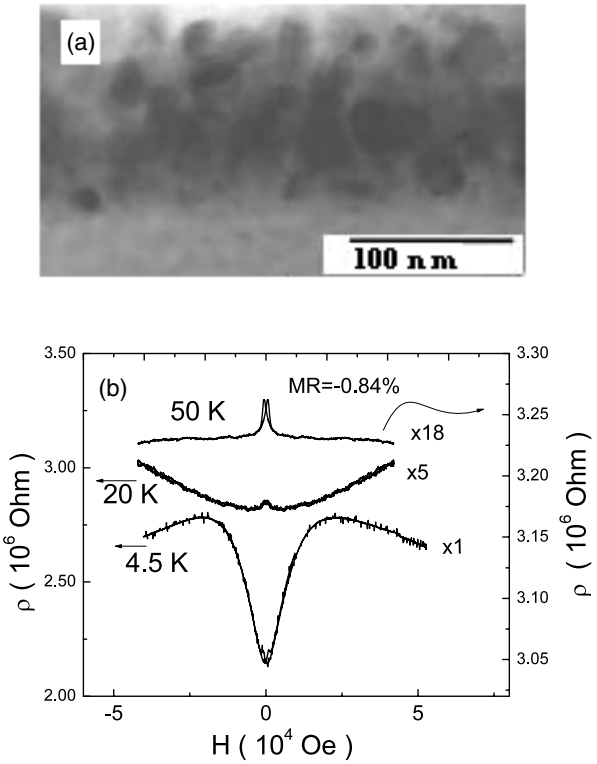

Figure 4. (a) The TEM image and (b) the ρ–H curve of the annealed $Zn_{0.28}Co_{0.72}O$ film (71 nm in thickness). The magnetoresistance was measured at 4.5, 20 and 50 K, respectively. In (b), the value of the sheet resistance at 50 K was multiplied by a factor of 18 (indicated by $\times 18$), and the value of the sheet resistance at 20 K was multiplied by a factor of five (indicated by $\times 5$).

low doping concentration, and the mechanism of the MR in these materials is not clear. But it is clear that the MR observed in the annealed sample in the high field region has no relation with the ferromagnetism of the annealed sample. Therefore, different MR behaviour between the annealed Co–ZnO metal–semiconductor granular films and the as-deposited $Zn_{1-x}Co_xO$ magnetic semiconductor films, in turn, indicates that the observed transport properties in the as-deposited magnetic semiconductor films are not related to the metal–semiconductor granular system.

In summary, electrical transport and magnetoresistance in the $Ti_{1-x}Co_xO_2$ and $Zn_{1-x}Co_xO$ magnetic semiconductors have been studied experimentally and theoretically. The spin-dependent variable range hopping model has been quantitatively established by taking into account the electron–electron Coulomb interaction and the spin–spin exchange interaction. The linear relation of $\ln \rho$ versus $T^{-1/2}$ in the low temperature range, which was observed experimentally to show different slopes and intersections at different magnetic fields, is well described by the spin-dependent variable range hopping model.

Acknowledgments

This work was supported by the Project 973 grant Nos 2001CB610603, NCET040634, and NSF grant Nos 10234010, 50102019 and 50572053.

References

[1] Mott N F 1969 *Phil. Mag.* **19** 835
[2] Efros A L and Shklovskii B I 1975 *J. Phys. C: Solid State Phys.* **8** L49
[3] Meir Y 1996 *Europhys. Lett.* **33** 471
[4] Kamimura H, Kurobe A and Takemori T 1983 *Physica* B **117** 652
[5] Shlimak I, Khondaker S I, Pepper M and Ritchie D A 2000 *Phys. Rev.* B **61** 7253
[6] von Molnar S, Briggs A, Flouquet J and Remenyi G 1983 *Phys. Rev. Lett.* **51** 706
[7] Oiwa A, Katsumoto S, Endo A, Hirasawa M, Iye Y, Ohno H, Matsukura F, Shen A and Sugawara Y 1998 *Phys. Status Solidi* b **205** 167
[8] Wagner P, Gordon I, Trappeniers L, Vanacken J, Herlach F, Moshchalkov V V and Bruynseraede Y 1998 *Phys. Rev. Lett.* **81** 3980
[9] Viret M, Ranno L and Coey J M D 1997 *Phys. Rev.* B **55** 8067
[10] Xiong P, Zink B L, Applebaum S I, Hellman F and Dynes R C 1999 *Phys. Rev.* B **59** R3929
[11] Fukuyama H and Yosida K 1979 *J. Phys. Soc. Japan* **46** 102
Yosida K and Fukuyama H 1980 *J. Phys. Soc. Japan* **48** 1879
Fukuyama H and Yosida K 1981 *Physica* B **105** 132
[12] Auslender M I, Kogan E M and Tretyakov S V 1988 *Phys. Status Solidi* b **148** 289
[13] Yan S S, Ren C, Wang X, Yan X, Zhou Z X, Mei L M, Ren M J, Chen Y X, Liu Y H and Garmestani H 2004 *Appl. Phys. Lett.* **84** 2376
[14] Song H Q, Mei L M, Yan S S, Ma X L, Liu J P, Yong Y and Zhang Z 2006 *J. Appl. Phys.* **99** 123903
[15] Han S J, Song J W, Yang C H, Park S H, Park J H, Jeong Y H and Rhie K W 2002 *Appl. Phys. Lett.* **81** 4212
[16] Fukumura T, Jin Z, Ohtomo A, Koinuma H and Kawasaki M 1999 *Appl. Phys. Lett.* **75** 3366
[17] Matsumoto Y, Murakami M, Shono T, Hasegawa T, Fukumura T, Kawasaki M, Ahmet P, Chikyow T, Koshihara S Y and Koinuma H 2001 *Science* **291** 854
[18] Shinde S R, Ogale S B, Sarma S D, Simpson J R, Drew H D, Lofland S E, Lanci C, Buban J P, Browning N D, Kulkarni V N, Higgins J, Sharma R P, Greene R L and Venkatesan T 2003 *Phys. Rev.* B **67** 115211
[19] Wang Z J, Tang J K, Tung L D, Zhou W L and Spinu L 2003 *J. Appl. Phys.* **93** 7870
[20] Sheng P, Abeles B and Arie Y 1973 *Phys. Rev. Lett.* **31** 44
[21] Kim J J and Lee H J 1993 *Phys. Rev. Lett.* **70** 2798
[22] Dietl T, Haury A and d'Aubigné Y M 1997 *Phys. Rev.* B **55** R3347
[23] Hamilton E M 1972 *Phil. Mag.* **26** 1043
[24] Inoue J and Maekawa S 1996 *Phys. Rev.* B **53** R11927
[25] Helman J S and Abeles B 1976 *Phys. Rev. Lett.* **37** 1429
[26] Mitani S, Takahashi S, Takanashi K, Yakushiji K, Maekawa S and Fujimori H 1998 *Phys. Rev. Lett.* **81** 2799
[27] Kennedy R J, Stampe P A, Hu E, Xiong P, von Molnar S and Xin Y 2004 *Appl. Phys. Lett.* **84** 2832
[28] Sheng P and Abeles B 1972 *Phys. Rev. Lett.* **28** 34
[29] Ogale S B, Choudhary R J, Buban J P and Lofland S E 2003 *Phys. Rev. Lett.* **91** 077205